SET 07 01 03

ABCM
Brazilian Society of Mechanical Sciences

Journal of the Brazilian Society of Mechanical Sciences

Published Quarterly by The Brazilian Society of Mechanical Sciences

VOLUME XXIV • NUMBER 1 • MARCH 2002

ABCM, Journal of Mechanical Science
The Journal of the Brazilian Society of Mechanical Sciences (ISSN 0100-7386) is published quarterly and owned by The Brazilian Society of Mechanical Sciences (ABCM), Avenida Rio Branco 124 18o Andar, 20040-001, Rio de Janeiro, Brazil, telephone (+5521) 2221 0438, email abcm@domain.com.br, and is distributed freely to members. Rate for 2002 is $320.00 for institutions and $120.00 to individuals. Issues are airmail shipped. All subscriptions are payable in advance and entered on an annual basis.

Indexed by Applied Mechanics Review and Engineering Information, INC.
Published by the Brazilian Society of Mechanical Sciences

TECHNICAL PAPERS

H. B. Coda
Escola de Engenharia de São Carlos
Universidade de São Paulo. Brazil
hbcoda@sc.usp.br

A Well Stated Time Domain Integral Representation for Elastodynamic Analysis and Applications

This article discusses three possible ways to derive time domain boundary integral representations for elastodynamics. This discussion points out possible difficulties found when using those formulations to deal with practical applications. The discussion points out recommendations to select the convenient integral representation to deal with elastodynamic problems and opens the possibility of deriving simplified schemes. The proper way to take into account initial conditions applied to the body is an interesting topict shown. It illustrates the main differences between the discussed boundary integral representation expressions, their singularities and possible numerical problems. The correct way to use collocation points outside the analyzed domain is carefully described. Some applications are shown at the end of the paper, in order to demonstrate the capabilities of the technique when properly used.
Keywords: *Elastodynamics, integral representations, boundary elements*

Introduction

The boundary element community has already seen many interesting studies on elastodynamics. One can see for instance: Antes & Steinfeld (1992), Mansur (1988), Kobayashi (1987), Coda et alli (1999a), Coda & Venturini (1999b), Domingues (1993) and Manolis (1986). This subject has attracted the attention of many researchers around the world. Very good reviews are given in the works of Beskos (1988) and Beskos (1997).

The present paper focus its discussion mainly on the Time Domain Boundary Element Method (TDBEM) applied to elastodynamic problems. As it is a well-known subject, the author intends to discuss the possible ways to derive time domain boundary integral representations for elastodynamics, pointing out the main differences among them, and their difficulties to present stable results. Another interesting topic discussed is how to deal with initial conditions for the different methodologies available. A straightforward way to couple the Finite Element Method to the Boundary Element Method is described, which allows the analysis of dynamic soil-structure interaction accurately and with numerical efficiency. The correct way to use external collocation points is also discussed. This discussion is important in order to clarify some properties of wave propagation problems that should be considered when using the TDBEM.

At the end of the paper some problems are solved using the smooth formulation, in order to show the applicability of the technique.

Nomenclature

Ω = *Studied domain*
Γ = *Boundary of the body*
σ_{ij} = *Stress tensor*
ε_{ij} = *Strain tensor*
u_i = *Displacement, i direction*
p_i = *Traction, i direction*
e = *smaller distance between outside source and boundary*
τ = *time*
C_1 = *Long. wave velocity*
C_2 = *Shear wave velocity*
$\sim$ = *Sotokes State*
$*$ = *Fundamental values*
ρ = *Density*
f = *Time function behaviour*
E = *Elasticity modulus*
ν = *Poisson's ratio*
b_i = *Body force, i direction*
$\partial^2 u / \partial \tau^2$ = *Acceleration*
$\ddot{u}$ = *Acceleration*
v = *velocity*
$\bar{}$ = *Prescribed values*
v_0 = *linitial value*
$H()$ = *Heaviside Function*
, = *Partial derivative*
$\delta()$ = *Dirac's delta distribution*

The Elastodynamic Problem

This section presents a summary of the elastodynamic equations. The formal achievement of these equations can be found in Achenbach (1975), Love (1944) and Erigen & Suhubi (1974).

The governing differential equation of linear elastodynamic equilibrium (i.e. the Navier-Cauchy equation) is given by

$$\left(C_1^2 - C_2^2\right) u_{j,ji} + C_2^2 u_{i,jj} + b_i / \rho = \ddot{u}_i \,, \qquad (1)$$

where b_i and u_i are body forces and displacements, respectively. Symbol ρ stands for the medium density, while C_1 and C_2 represent longitudinal and shear wave propagation velocities, respectively.

Equation (1) can also be written in terms of stresses σ_{ij}, as follows,

$$\sigma_{ij,i} + b_j = \rho \frac{\partial^2 u_j}{\partial t^2} = \rho \ddot{u}_j \,. \qquad (2)$$

Assuming the problem defined over a domain Ω with boundary Γ, the following boundary conditions along time have to be specified:

$$\begin{cases} u_i(x,t) = \bar{u}_i(x,t) & x \in \Gamma_1 \\ p_i(x,t) = \bar{p}_i(x,t) & x \in \Gamma_2 \end{cases}, \qquad (3)$$

Manuscript received: March, 2001. Technical Editor: José Roberto F. Arruda

where $p_i(x,t)$ represents the boundary tractions obtained from the stress field using the Cauchy's formulae and $\Gamma = \Gamma_1 \cup \Gamma_2$.

As usual, the initial conditions are given by

$$\begin{cases} u_i(x,t_0) = u_{i0}(x) \\ \\ \dot{u}_i(x,t_0) = v_{i0}(x) \end{cases} \qquad x \in \Omega \,. \tag{4}$$

Graffi's Reciprocal Theorem

Following the weighting residual technique steps given in the studies of Mansur (1985), Coda (1993), Araújo (1994), Domingues (1993) and Coda (2000a), one can achieve Graffi's reciprocal theorem from eq. (2), as follows:

$$\begin{aligned} &\int_{t_0}^{t}\int_{\Omega} u_j(\tau)\tilde{b}_j(t-\tau)d\Omega d\tau + \int_{t_0}^{t}\int_{\Gamma} u_j(\tau)\tilde{p}_j(t-\tau)d\Gamma d\tau = \\ &\int_{t_0}^{t}\int_{\Gamma} p_j(\tau)\tilde{u}_j(t-\tau)d\Gamma d\tau + \\ &+ \int_{t_0}^{t}\int_{\Omega} b_j(\tau)\tilde{u}_j(t-\tau)d\Omega d\tau + \int_{t_0}^{t}\int_{\Omega}\sigma_{ij}^{a}(\tau)\tilde{\varepsilon}_{ij}(t-\tau)d\Omega d\tau + \\ &+ \int_{\Omega}\rho\{\dot{u}_j(\tau)\tilde{u}_j(t-\tau) - u_j(\tau)\dot{\tilde{u}}_j(t-\tau)\}\Big|_{t_0}^{t} d\Omega \end{aligned} \tag{5}$$

where $\{\tilde{u}_i(\tau),\tilde{\sigma}_{ij}(\tau)\}$ is weighting field, $\{u_i(\tau),\sigma_{ij}(\tau)\}$ represents the actual solid displacement and stress fields, while $\sigma_{ij}^{a}(\tau)$ stands for the initial stress state. Particular attention is given to the last term in eq. (5) representing the initial conditions.

Boundary Integral Representation for Displacements

The boundary integral representation for displacements can be achieved from eq. (5) adopting a particular distribution for the weighting field body force, given by Wheeler and Sternberg (1968) as:

$$b_{kj}^{*} = \delta(s-q)\delta_{kj} f(\tau)\,, \tag{6}$$

where $\delta(s-q)$ is Dirac's delta distribution, 's' and 'q' represent the source and field points, δ_{kj} stands for the Kronecker delta, while $f(\tau)$ gives the time behavior of this set of loads.

For this particular body force distribution the weighting field $\{\tilde{u}_{ki}(\tau),\tilde{\sigma}_{kij}(\tau)\}$ represents the general Stokes' state. The general Stokes' state expression can be found, for example, in Wheeler & Sternberg (1968), Coda (1993), Karabalis & Beskos (1984), Kobayashi (1987), Mansur (1985) Domingues (1993) and Erigen & Suhubi (1974). Replacing Stokes' state and expression (6) into eq. (5) yields the following integral representation:

$$\begin{aligned} &C_{ki}(Q,s)\int_{t_0}^{t} u_i(s,\tau)f(t-\tau)d\tau + \int_{t_0}^{t}\int_{\Gamma} u_j(\tau)\tilde{p}_{kj}(Q,t;s|f(\tau))d\Gamma d\tau = \\ &\int_{t_0}^{t}\int_{\Gamma} p_j(\tau)\tilde{u}_{kj}(Q,t,s|f(\tau))d\Gamma d\tau + \int_{t_0}^{t}\int_{\Omega} b_j(\tau)\tilde{u}_{kj}(Q,t,s|f(\tau))d\Omega d\tau + \\ &\int_{t_0}^{t}\int_{\Omega}\sigma_{ij}^{a}(\tau)\tilde{\varepsilon}_{kij}(Q,t,s|f(\tau))d\Omega d\tau + \\ &\int_{\Omega}\rho\{\dot{u}_j(\tau)\tilde{u}_{kj}(Q,t,s|f(\tau)) - u_j(\tau)\dot{\tilde{u}}_{kj}(Q,t,s|f(\tau))\}\Big|_{t_0}^{t} d\Omega \end{aligned} \tag{7}$$

From eq. (7) one can obtain three main alternatives to write a displacement integral representation.

The first alternative can be seen, for instance, in Kobayashi (1987), Mansur (1985) and Manolis (1986). It is an elegant way to obtain the desired representation. This approach consists in replacing, in eq. (7), the time function $f(\tau)$ by Dirac's delta distribution. Thus, assuming $f(\tau) = \delta(\tau)$ to represent the body force distribution b_{kj}^{*}, eq. (6), results in

$$\begin{aligned} &C_{ki}(Q,s)u_i(s,t) = \int_{t_0}^{t}\int_{\Gamma} u_{ki}^{*}(Q,t;s,\tau)p_i(Q,\tau)d\Gamma d\tau + \\ &- \int_{t_0}^{t}\int_{\Gamma} u_i(Q,\tau)p_{ki}^{*}(Q,t;s,\tau)d\Gamma d\tau + \\ &\int_{t_0}^{t}\int_{\Omega} u_{ki}^{*}(q,t;s,\tau)b_i(q,\tau)d\Omega d\tau \\ &\int_{t_0}^{t}\int_{\Omega}\sigma_{ij}^{a}(\tau)\varepsilon_{kij}^{*}(Q,t;s,\tau)d\Omega d\tau + \\ &\int_{\Omega}\rho\{\dot{u}_j(\tau)u_{kj}^{*}(Q,t;s,\tau) - u_j(\tau)\dot{u}_{kj}^{*}(Q,t;s,\tau)\}\Big|_{t_0}^{t} d\Omega\,, \end{aligned} \tag{8}$$

where field $\{u_{ki}^{*}(\tau),\sigma_{kij}^{*}(\tau)\}$ represents Dirac's delta fundamental solution.

Equation (8) is called here the *First Dirac's delta Displacement Integral Representation* or simply, *Loves' Identity* (LI) (Wheeler & Sternberg (1968) and Erigen & Suhubi (1974)).

Another way to derive a displacement integral representation can be found in Karabalis & Beskos (1984). As described for the previous procedure it consists in applying Dirac's delta distribution in expression (7), to find equation (8). After finding equation (8), Karabalis & Beskos (1984) applied a well-known Dirac's delta fundamental solution property, Eringen & Suhubi (1974), in order to write eq. (8) in a more compact form. The property mentioned is that the convolution between Dirac's delta fundamental solution and any other function results in a Stokes' state exhibiting the impulse distribution governed by the adopted function behavior. Following the above description, eq. (8) is rewritten as

$$\begin{aligned} &C_{ki}(Q,s)u_i(s,t) = \int_{\Gamma} u_{ki}^{0}(Q,t,s|p_i(Q,t))d\Gamma \\ &- \int_{\Gamma} p_{ki}^{0}(Q,t,s|u_i(Q,t))d\Gamma \end{aligned}$$

$$+\int_{\Omega} u^{0}_{ki}(Q,t,s|b_i(Q,t))d\Omega + \int_{\Omega} \varepsilon^{0}_{kij}(Q,t,s|\sigma^{a}_{ij}(Q,t))d\Omega +$$

$$\int_{\Omega} \rho\{\dot{u}_j(\tau)u^{*}_{kj}(Q,t;s,\tau) - u_j(\tau)\dot{u}^{*}_{kj}(Q,t;s,\tau)\}\Big|^{t}_{t0} d\Omega \,, \tag{9}$$

where field $\{u^{0}_{ki}(\tau), \sigma^{0}_{kij}(\tau)\}$ is the Stokes' state related to the behavior of the unknown variables $\{u, p\}$. Field $\{u^{*}_{ki}(\tau), \sigma^{*}_{kij}(\tau)\}$, present in the initial conditions term, is Dirac's delta fundamental solution, as stated in equation (8).

Note that Dirac's delta fundamental solution remains in the initial condition term, as the same weighting function has been used to achieve both eqs. (8) and (9). Equation (9) is named here the *Second Dirac's delta Displacement Integral Representation*, or simply the *Compact Loves' Identity* (CLI). It should be noted that in Eringen & Suhubi (1974) the Conpact Loves' Identity is called simply Loves' Identity. Although from a mathematical point of view there is no difference between eqs (9) and (8), in a numerical approach there is a difference regarding time approximation (see section 5).

More recently, Coda (1993, 2000a) and Coda and Venturini (1995a, 1995b, 1996a, 1996b, 1996c, 1999a and 1999b) worked on the subject trying to find a more stable procedure for the TDBEM. The way found by the authors to improve the TDBEM stability was obtained by reducing the kernel's singularities regarding time. Instead of assuming an instantaneous impulse, $b^{*}_{kj} = \delta(s-q)\delta_{kj}\delta(\tau)$, one starts by replacing $\delta(\tau)$ by the Heaviside distribution. The weighting function adopted to derive the integral representation is therefore, given by a concentrated load distributed over a time interval (Δt), as follows:

$$b^{*}_{ki} = [H(\tau) - H(\tau - \Delta t)]\delta(q-s)\delta_{ki} / \Delta t \,. \tag{10}$$

One can also choose smoother distributions, depending on the singularity reduction needed. Another possible formula to represent b^{*}_{kj} is given by

$$f(\tau) = \frac{g(\tau) - g(\tau - R_d * R_t)}{R_d}, \tag{11a}$$

with

$$g(\tau) = \left[56\left(\frac{\tau}{R_t} - \frac{1}{2}\right)^{7} - 36\left(\frac{\tau}{R_t} - \frac{1}{2}\right)^{5} + \frac{11}{2}\left(\frac{\tau}{R_t} - \frac{1}{2}\right)^{3} + \frac{\tau}{R_t}\right] \frac{[H(\tau) - H(\tau - R_t)]}{R_t} + \frac{H(\tau - R_t)}{R_t} \tag{11b}$$

where R_t is a sub-element of Δt defining the time that the load function requires to reach its maximum value and R_d is the duration of the load function at its maximum value ($2*R_t+R_d = \Delta t$).

Adopting the fundamental solution derived by choosing b^{*}_{kj} given by eq. (10) or (11) Graffi's theorem gives

$$C_{ki}(Q,s)\hat{u}_i(s,\Delta t) + \int_{t_0}^{t}\int_{\Gamma} u_j(\tau)\bar{p}_{kj}(Q,t;s|f(\tau))d\Gamma d\tau =$$

$$\int_{t_0}^{t}\int_{\Gamma} p_j(\tau)\bar{u}_{kj}(Q,t,s|f(\tau))d\Gamma d\tau +$$

$$+ \int_{t_0}^{t}\int_{\Omega} b_j(\tau)\bar{u}_{kj}(Q,t,s|f(\tau))d\Omega d\tau +$$

$$\int_{t_0}^{t}\int_{\Omega} \sigma^{a}_{ij}(\tau)\bar{\varepsilon}_{kij}(Q,t,s|f(\tau))d\Omega d\tau +$$

$$+ \int_{\Omega} \rho\{\dot{u}_j(\tau)\bar{u}_{kj}(Q,t,s|f(\tau)) - u_j(\tau)\dot{\bar{u}}_{kj}(Q,t,s|f(\tau))\}\Big|^{t}_{t_0} d\Omega \tag{12}$$

where $\hat{u}_i(s,\Delta t) = \int_{t-\Delta t}^{t} u_i(s,\tau)f(t-\tau)d\tau$ is understood as an average displacement value over the final time step. When a time approximation is assumed, this value becomes the time parametric displacement. Field $\{\bar{u}_{ki}(\tau), \bar{\sigma}_{kij}(\tau)\}$ is a Stokes' state related to the time load function given in either eq. (10) or (11).

The elastodynamic state achieved assuming the impulse distributed along a time interval is named here smooth fundamental solution. Note that this smooth fundamental solution is present in the initial conditions term in eq. (12).

As Dirac's delta fundamental solution has not been used to achieve expression (12), this representation is named here the *Smooth Displacement Integral Representation*, or simply *Smooth Loves' Identity* (SLI), Coda (2000a, 2000b).

Equations (8) and (9) were obtained using the same weighting function, i.e. Dirac's delta fundamental solution, therefore they present the same singularities. The difference between them is the convolution concerning time application order. In eq. (9) the time convolution is applied before imposing time approximation, while for eq. (8) the time convolution is applied after imposing time approximation.

It is accepted but not mentioned in literature that formulations based on eqs (8) and (9) are strongly unstable. Even after some regularization studies carried out by Siebrits & Pierce (1997) and Risos & Karabalis (1997) using spline functions, and Yu et all (1999) proposing a linear θ methodology, the theoretical evidences for instability turn the numerical calibration of results almost a try and error technique, disregarding generality. Some researchers have started to use the SLI in two-dimensional analysis, as it can be seen in Carrer & Mansur (2001).

Discussions about Integral Representations

The previous section presents three different integral representations to build the TDBEM, namely LI, CLI and SLI. Before describing how to develop the algebraic processes, which are practically the same in spite of the adopted integral representation, a discussion about the main differences among the three alternatives shall be presented, along with their main advantages and disadvantages.

A clear difference among representations described concerns the way of treating the initial conditions.

One can observe that in the three-dimensional LI and CLI integral representations (eqs. (8) and (9)), Dirac's delta fundamental

solution is present in the last volume integral in its displacement and velocity values. One can see from the fundamental solution expressions, Karabalis & Beskos (1984) or Wheeler & Sternberg (1968), that Dirac's delta distribution ($\delta(\ )$) and its derivative concerning time ($\dot{\delta}(\ )$) are present in the kernel of the volume integral mentioned.

As far as the author's knowledge goes, there is only a study of three-dimensional elastodynamic analysis, Antes & Steinfeld (1992), where the third integral of eq. (9), i.e. body weight integral, is performed. This integral is less singular when compared with the initial conditions one, but in that study, as the body weight is constant over time, this integral presents a Dirac's delta function (3D) and spherical surfaces should be integrated to fulfill the jump conditions requirements.

The subject of initial conditions in two-dimensional elastodynamics is treated by Sladek & Sladek (1992). Although Sladek & Sladek (1992) presented a mathematical discussion on the subject no practical results were presented, leading to no conclusions about stability.

When applying the Smooth Love's Identity (SLI), eq. (12), the initial velocity field is considered without problems, as in Coda & Venturini (1996a) and Coda(2000a). Initial displacement can be treated adopting at least a piecewise linear fundamental load function, Coda (2000a). In order to obtain a stable procedure for general problems, one should adopt at least a load function of class C^1. It should be mentioned that Carrer & Mansur (2001) used SLI to solve initial conditions for two-dimensional scalar wave propagation problems.

Another difference between Smooth Integral Representations and the ones based on the Dirac's delta fundamental solution is related to their behavior when constant time approximation is assumed (3D).

First of all, the difference between eqs. (8) and (9), which are apparently the same, is clearly noted when constant time approximation is adopted. It is impossible to impose constant time approximation for displacements in eq. (8) as the first derivative of Dirac's delta is present in the Kernel of the first integral on the right side of eq. (8). It indicates that the result of this convolution is the time derivative of the constant function (approximation), resulting in no contribution of this term and leading to instability of the resulting numerical process. From this assumption, one concludes that it is necessary, for LI (3D), at least a linear time approximation for displacements.

If displacements are taken as constant over a time step in eq. (9), the considered kernels will represent distributed impulses along time steps and generate kernels that necessarily contain Dirac's delta distributions. Following this assumption, one concludes that the approximated Compact Love's Identity has been obtained in an incomplete way. In order to correct this mistake the creation of spherical surfaces inside the body to guarantee the well known "jump conditions", is necessary. In studies based on CLI, as Karabalis & Beskos (1984), these considerations have not been made, resulting in unstable algorithms. It is also noted, that for free surface problems, where the problematic kernel (surface fundamental tractions) has no influence, the CLI deficiencies will not be evident.

It is very simple to verify that when using SLI based on Heaviside fundamental solution, eq. (10), the application of constant time approximation for both displacements and tractions satisfies completely Graffi's theorem, (Wheeler & Sternberg (1967)), leading to a consistent and stable procedure. The numerical technique based on SLI has presented very good results in various studies, Coda and Venturini (1995-1999), and some new results are presented here, coupled and not coupled with finite element models. It is worth noting that by analyzing all the questions about classical formulations based on LI or CLI, they can be safely used with additional effort on the quality of numerical integration procedures, Araujo et all (1999). For stress integral representations the difficulties are worse, as the time singularities of the kernels are increased one time.

The discussion carried out was based on three-dimensional expressions. For two-dimensions the kernel singularities concerning time are smaller than for three-dimensions, but in general the integral formulation behavior is similar, Mansur et all (2001) and Mansur (1985).

External Collocation Points

In literature it is usual to find references to the direct application of exterior source points in eqs (8) and (9), assuming the free term to be zero, i.e., "$C_{kj} = 0$", as for the static case, see Kobayashi (1987). Following this proposition it is impossible to implement a stable non-singular TDBEM. This section describes the way to correctly write integral representations for external collocation points.

In order to understand what is proposed it is necessary to keep in mind the wave motion characteristics of the fundamental solution. The elastic waves move in two fronts with distinct velocities C_1 (longitudinal waves) and C_2 (shear waves), being "$C_1 > C_2$". After some period of time 't' from the application of the concentrated load on source 's', a certain region of the medium has suffered a perturbation. In figure 1, the hatched area represents the disturbed region.

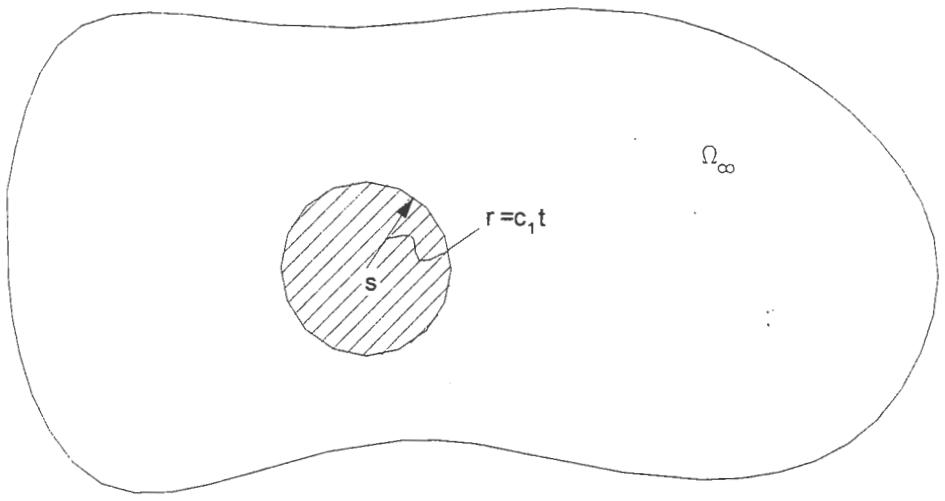

Figure 1. Disturbed region after a period of time 't' due to the concentrated force in 's'.

Points outside this region do not suffer the influence of the load. When the load point is inside domain or over boundary the convolution described by eqs (8), (9) and (12) can be shown schematically as in figure 2.

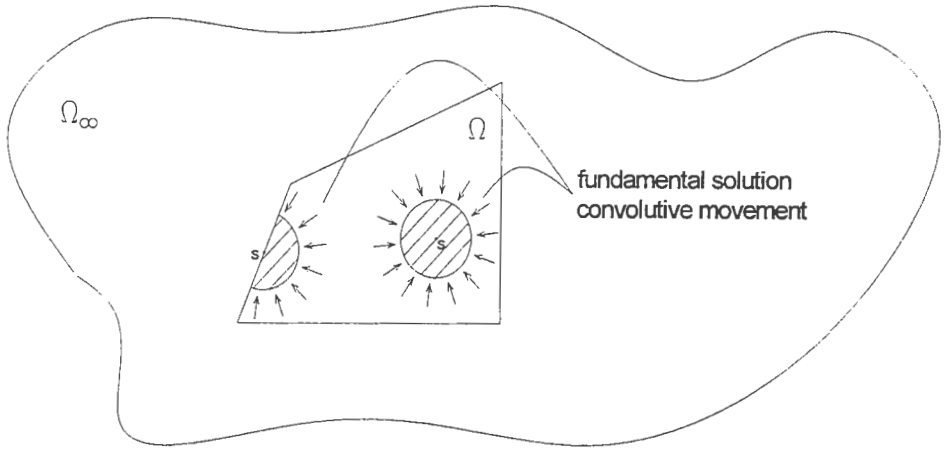

Figure 2. Graphical convolution scheme.

One should realize that, as in the convolution process the fundamental values are written in terms of $(t-\tau)$, the external radius of the hatched regions of figure 2 represents the initial instant, i.e., '0'. Similarly, the perturbation end is at point 's' for instant 't'.

When the possibility of putting the source point outside the studied body is supposed, the usual procedure leads to draw the schematic representation of figure 3.

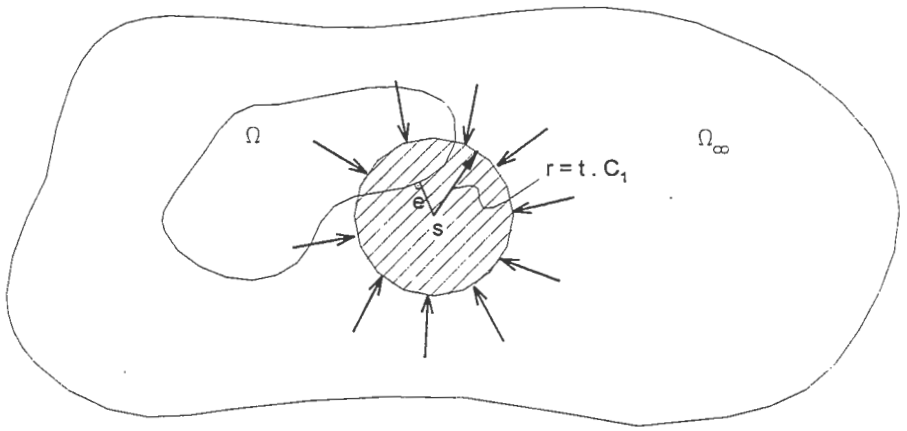

Figure 3. Erroneous representation of the convoluting process.

The algebraic representation (neglecting initial conditions and body forces), related to this erroneous procedure comes from equation (7) (or even (8), (9) and (12)) and is written as:

$$\int_\Gamma \int_0^t p^*_{kj}(Q,t-\tau;s/f)u_j(\tau)d\tau d\Gamma = \int_\Gamma \int_0^t u^*_{kj}(Q,t-\tau;s/f)p_j(\tau)d\tau d\Gamma \tag{13}$$

Equation (13) can be divided into two parts, as follows:

$$\int_\Gamma \int_0^{(t-e/c_1)} p^*_{kj}(Q,t-\tau;s/f)u_j(\tau)d\tau d\Gamma + \int_\Gamma \int_{(t-e\ c_1)}^t p^*_{kj}(Q,t-\tau;s/f)u_j(\tau)d\tau d\Gamma = \int_\Gamma \int_0^{(t-e/c_1)} u^*_{kj}(Q,t-\tau;s/f)p_j(\tau)d\tau d\Gamma + \int_\Gamma \int_{(t-e/c_1)}^t u^*_{kj}(Q,t-\tau;s/f)u_j(\tau)d\tau d\Gamma, \tag{14}$$

where 'e' is the smaller distance between 's' and Γ.

The meaning of eq. (14) can be seen in figure 4.

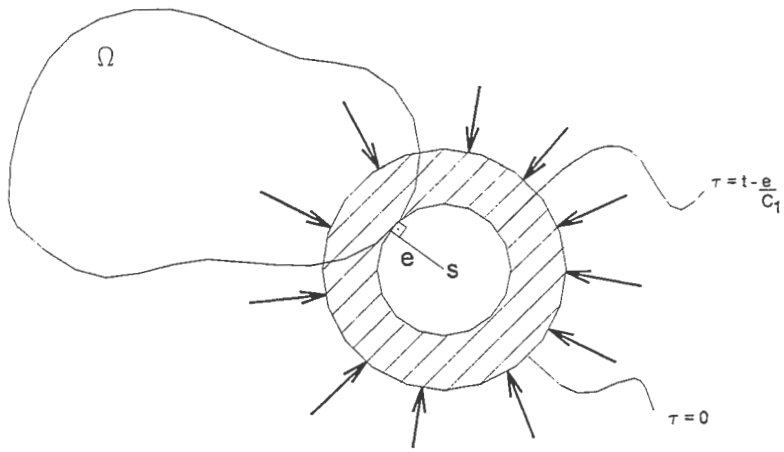

Figure 4a. Spreading of the erroneous integral representation, interval [0, t – e/c1].

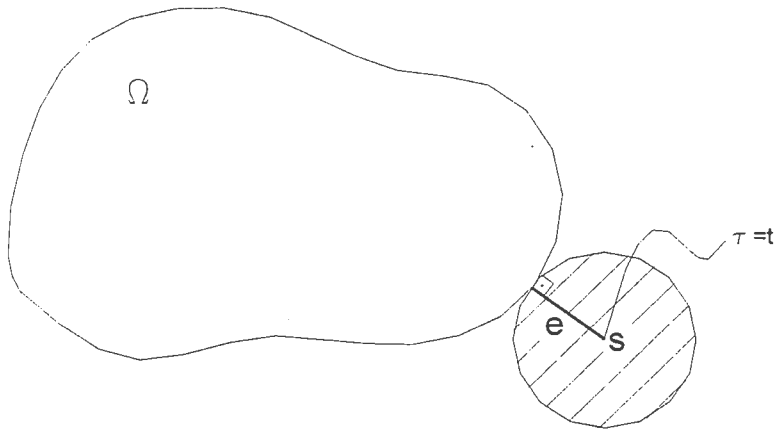

Figure 4b. Spreading of the erroneous integral representation, interval [t – e/c_1, t].

It is easy to note that during the interval [t – e/C_1,t] there is no presence of the fundamental values in eq. (13) and, therefore, part of the convoluting process is lost, which makes this representation worthless.

On the other hand, if one starts from part of eq. (14) where the fundamental solution is not zero,

$$\int_\Gamma \int_0^{(t-e\ c_l)} p^*_{kj}(Q,t-\tau;s/f)u_j(\tau)d\tau d\Gamma = \int_\Gamma \int_0^{(t-e\ c_l)} u^*_{kj}(Q,t-\tau;s/f)p_j(\tau)d\tau d\Gamma\ , \qquad (15)$$

it is possible to write a valid integral representation for external sources. This is done applying a time translation of the final instant of analysis. For that sake, let us define

$$t' = t - e/C_1\ , \qquad (16)$$

and, therefore,

$$t = t' + e/C_1\ , \qquad (17)$$

Then, substituting expression (17) in eq. (15) results:

$$\int_\Gamma \int_0^{t'} p^*_{kj}(Q,t'+e/C_l-\tau;s/f)u_j(\tau)d\tau d\Gamma = \int_\Gamma \int_0^{t'} u^*_{kj}(Q,t'+e/C_l-\tau;s/f)p_j(\tau)d\tau d\Gamma\ . \qquad (18)$$

Equation (18) means that the convoluting process, for outside sources, should be carried out by means of time translated fundamental values.

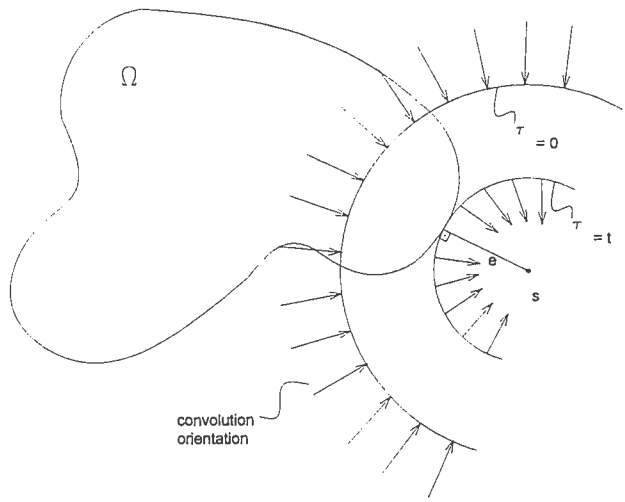

Figure 5. Correct convoluting process along interval [0,t].

The scheme of this procedure can be seen in figure 5 and the complete eq. (12) is given by:

$$\int_0^t \int_\Gamma p^*_{kj}(Q,t+\frac{e}{C_l}-\tau;s/f)u_j(\tau)d\Gamma d\tau +$$

$$\int_\Omega \rho u_j(0)\dot{u}^*_{kj}(q,t+\frac{e}{C_l};s/f)d\Omega =$$

$$\int_0^t \int_\Gamma u^*_{kj}(Q,t+\frac{e}{C_1}-\tau;s/f)p_j(\tau)d\Gamma d\tau + +$$

$$\int_0^t \int_\Omega u^*_{kj}(q,t+\frac{e}{C_l}-\tau;s/f)b_j(\tau)d\Omega d\tau +$$

$$\int_0^t \int_\Omega \varepsilon^*_{kij}(q,t+\frac{e}{C_l}-\tau;s/f)\sigma^n_{ij}(\tau)d\Omega d\tau$$

$$+ \int_\Omega \rho \dot{u}_j(0)u^*_{kj}(q,t+\frac{e}{C_l};s/f)d\Omega . \qquad (19)$$

Equation (19) is the correct version of eq. (12) for outside point collocation.

Algebraic Process and the Finite Element Method

The steps to transform either eq (12) or (19) into an algebraic system of equations can be found in any good reference of TDBEM, as for example, Mansur (1983), Domingues (1993), Kobayashi (1987), Araujo (1994), Coda (1993) and Coda (2000a). Following these steps one finds:

$$H^{n_t}_{\theta\beta}\ U_{\theta\beta} = G^{n_t}_{\theta\beta}\ P_{\theta\beta} + B^{n_t}_{\theta\beta}\ b_{\theta\beta} + Q^{n_t}_{\theta\beta}\ \sigma^n_{\theta\beta} + W^{n_t}\ V_0 , \qquad (20)$$

where the superscript n_t represents the final instant of all convoluting process related to the instant of interest. Indices θ and β represent the time interval approximation considered. Thus one has a summation from 1 to n_t in θ and a summation from 1 to the time approximation order in β.

Expression (20) can be written, for any final convoluting instant, in a compact form as follows:

$$HU = GP + F \qquad (21)$$

where F contains the history of the movement.

Following a weighting residual procedure allied to a spatial approximation technique and a time integrator, as for example Newmark β, one can write the following linear equation system in order to represent the dynamic equilibrium equation at any instant. (Finite Element Method, Bathe (1980))

$$K^f U = G^f P + F^f , \qquad (22)$$

where superscript "f" represents finite element.

Coupling

In order to make the coupling between BEM and FEM the sub-region technique is adopted, Coda & Venturini (1995, 1999a, 1999b) and Beer & Watson (1992).

Taking two sub-regions defined by Ω_i and Ω_j, which are coupled with each order by means of interface Γ_{ij}, one applies eqs (21) and (22) for each body, resulting in

$$H^i U^i = G^i P^i + A^i , \qquad (23)$$

$$H^j U^j = G^j P^j + A^j . \qquad (24)$$

Equations (23) and (24) are written for a single instant. Despite the occurrence of repeated indices in expressions (23) and (24) it does not imply summation.

Both equilibrium and kinematical compatibility conditions along interface Γ_{ij} are written as:

$$U^{ij} = U^{ji} , \qquad (25)$$

$$P^{ij} = -P^{ji} , \qquad (26)$$

where the superscripts represent the first and the second contact sub-region, respectively.

U^{ij} and P^{ij} values are respectively, the displacement and the traction along the contact surfaces. The values that do not belong to the contact surface are called U^{ie} and P^{ie}. Substituting eqs. (25) and (26) in eqs (23) and (24), results in

$$\begin{bmatrix} H^{ie} & H^{ij} & -G^{ij} & 0 \\ 0 & H^{ji} & G^{ji} & H^{je} \end{bmatrix} \begin{Bmatrix} U^{ie} \\ U^{ij} \\ P^{ji} \\ U^{je} \end{Bmatrix} = \begin{bmatrix} G^{ie} & G^{ij} & 0 & 0 \\ 0 & 0 & G^{je} & G^{ji} \end{bmatrix} \begin{Bmatrix} P^{ie} \\ \overline{P}^{ij} \\ P^{je} \\ \overline{P}^{ji} \end{Bmatrix} + \begin{Bmatrix} A^i \\ A^j \end{Bmatrix} \qquad (27)$$

where $\overline{P}^{ij}$ represents the prescribed values on the contact surface This expression can be easily extended to an arbitrary number of sub-regions, see for instance Coda & Venturini (1999a), Coda et all (1999b) and Coda (2000a)

Numerical Examples

In this section some new examples are shown applying the SLI formulation. The fundamental solution adopted is defined by the load function of equation (10). No comparisons with other results are shown in this paper. Differences between SLI formulation and LI (or CLI) regarding stability and accuracy can be seen in Coda & Venturini (1996c) for three-dimensional problems.

Regarding computational effort one concludes that for three-dimensional analysis the formulations based on SLI are more economic than the classical ones. It occurs as it is possible to apply constant time approximations for displacements employing SLI, while it is not a good choice in CLI or LI formulations. It is obvious that when applying the same approximations for all schemes, LI or CLI is more economic than SLI for three-dimensional problems. It occurs because the smooth fundamental solutions wave fronts have larger width than the one of Dirac's delta. For two-dimensional analysis the computational effort is the same (when using the same approximation), as the fundamental solutions values do not vanish after some period of time.

Spherical Cavity under a Loaded Half Space

For the analysis of the half space, shown in figure 6, two situations will be considered. The first one consists in applying the load over the free surface without including anything under the loaded surface to verify if the solution converges to the static result. Then a spherical cavity with radius r=2.5m is placed under the loaded surface. Its center is located at x_3 axis, 5m beyond the loaded surface. The influence of the spherical cavity, regarding displacement and stress intensity for selected points is studied. In figure 6, the intensity, shape and time behaviour of the external load

are shown. The physical constants are $E = 2.10^8 Kg/(ms^2)$, $\nu = 0,25$, $\rho = 1600kg/m^3$ and $\Delta t = 0,0085s$.

As Stokes' fundamental solution is applied and internal displacements and stresses are of interest, it is necessary to discretize an extension of the free surface, figure 7. Both vertical displacement and vertical stress component σ_{33} for points A (0,0,0), B (0,0,5), C (10,0,5), D (0,0,15) and E (10,0,15), without the spherical cavity consideration, are shown in figure 8. compressive stresses were represented as positive.

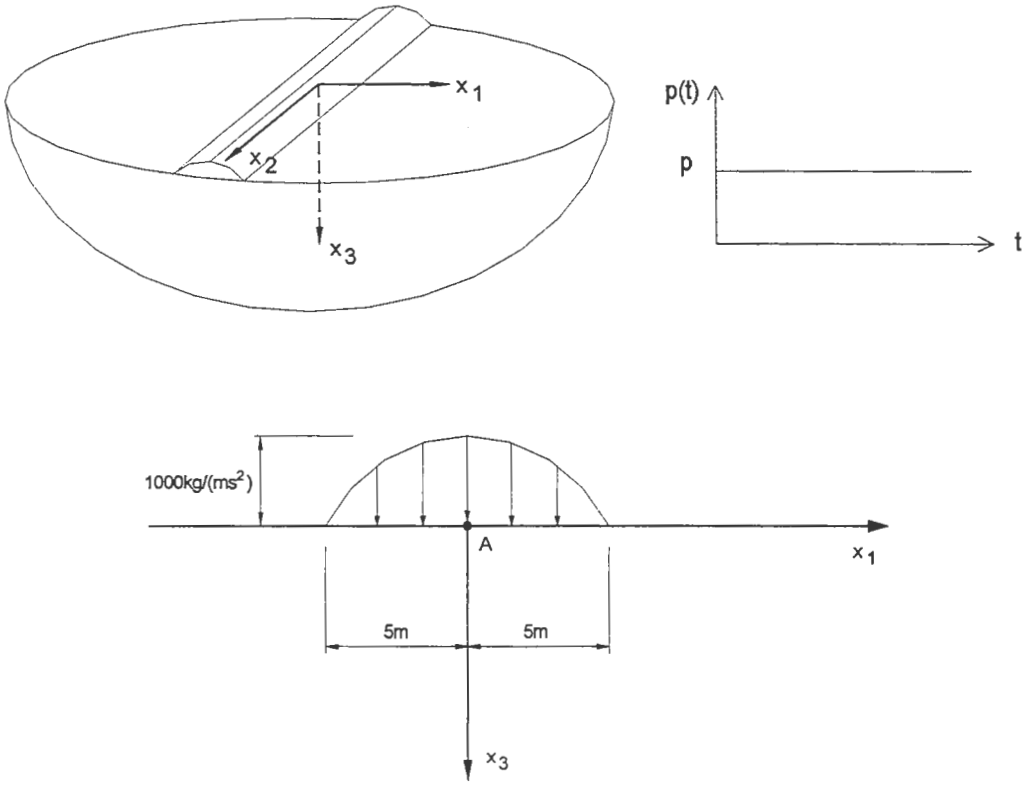

Figure 6. Half space and applied load.

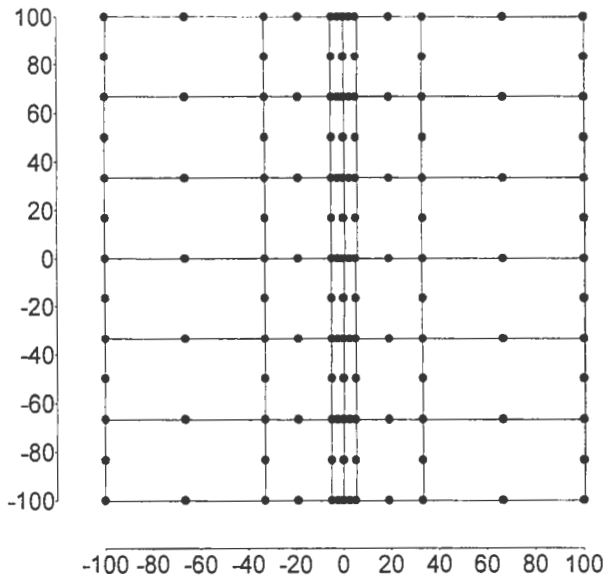

Figure 7. Surface discretization.

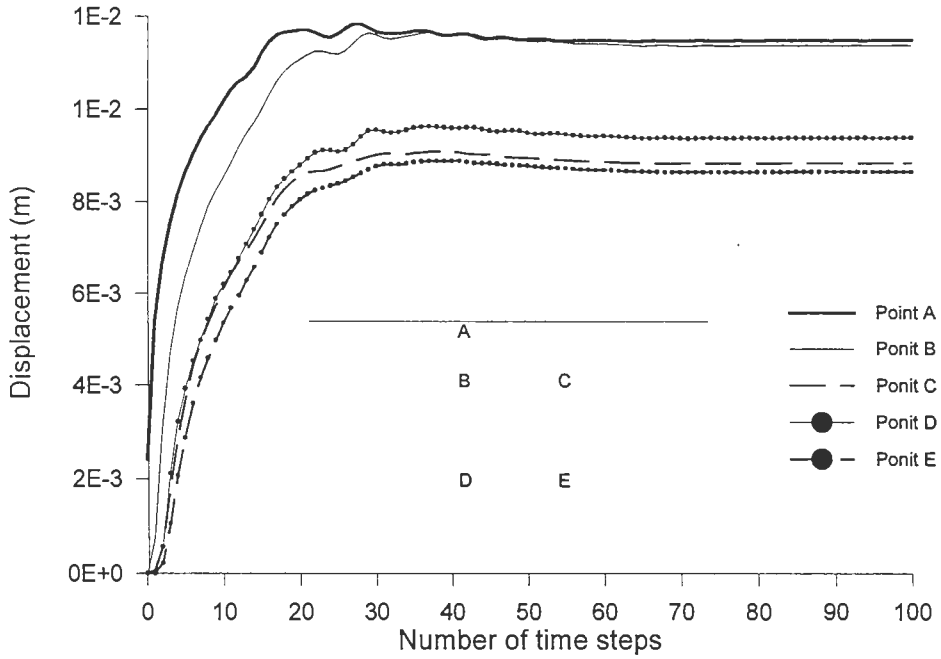

Figure 8a. Displacement at points A, B, C, D and E for the adopted loading.

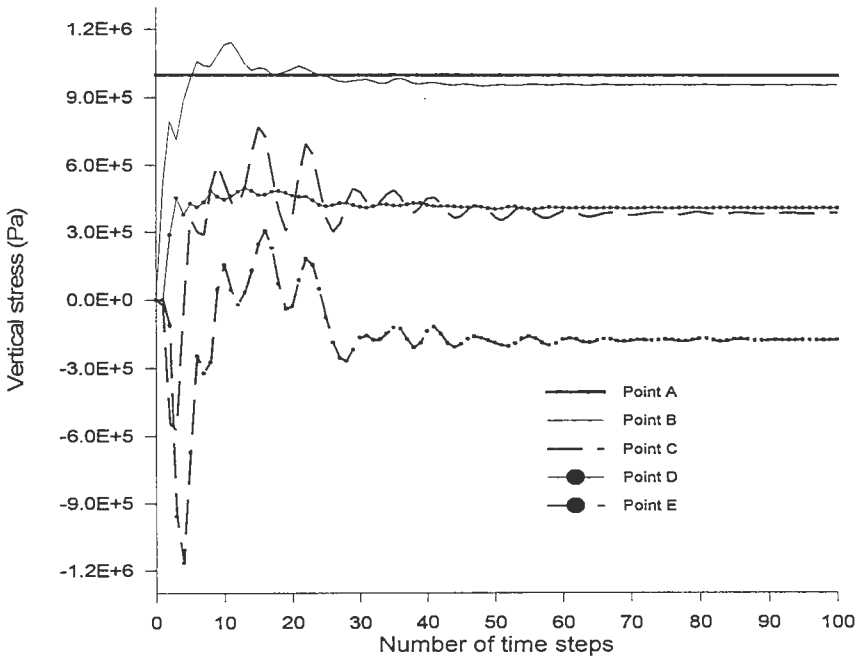

Figure 8b. Stress component σ33 for points A, B, C, D and E for the adopted loading.

The results are stable and converge to the static values, as expected.

Now, consider a spherical cavity placed under the loaded surface with radius R=2.5m and centred at point B, exactly between the load and point D as illustrated in figure 8a. Again vertical displacements and σ_{33} stresses are analyzed for points A, D, E as well as for an auxiliary point (0,0,8), see figures 9 and 10. A total of fifty four (54) quadratic isoparametric boundary elements were used to model the spherical cavity.

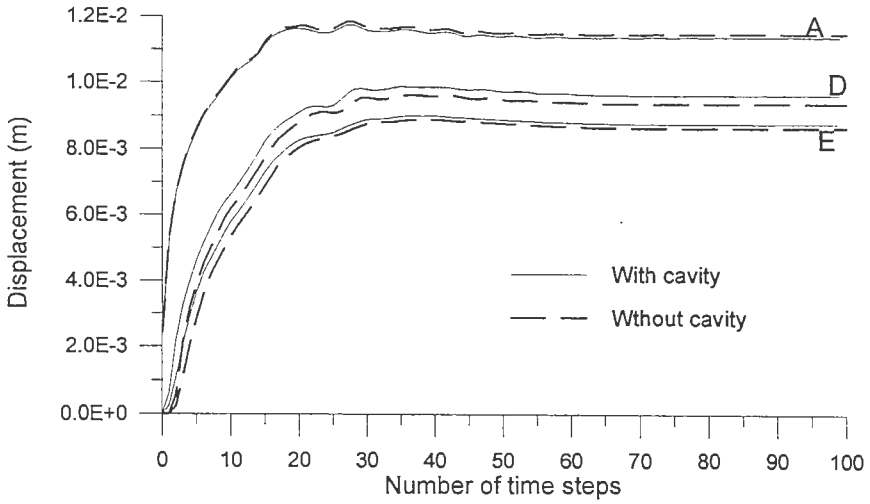

Figure 9a. Vertical displacement at points A, D and E.

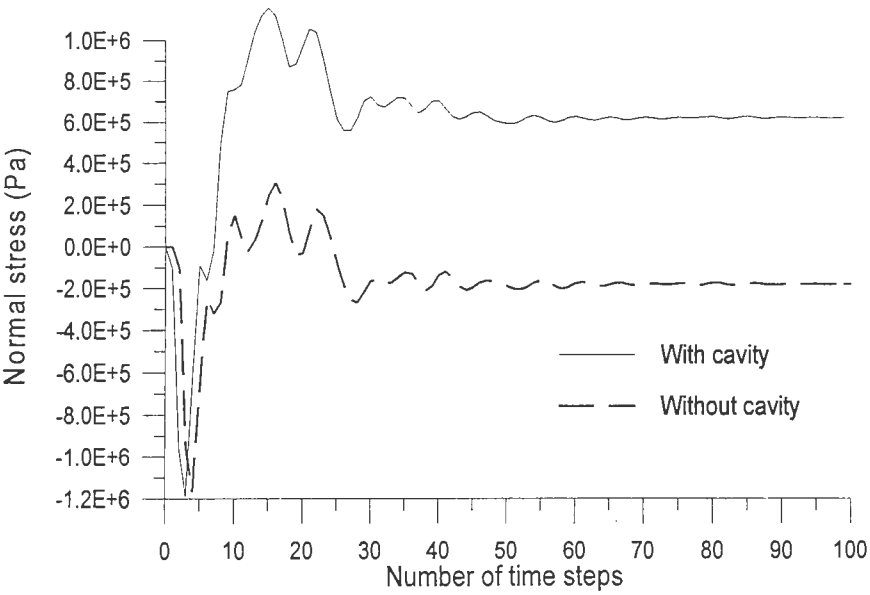

Figure 9b. Stress component σ33 at point E.

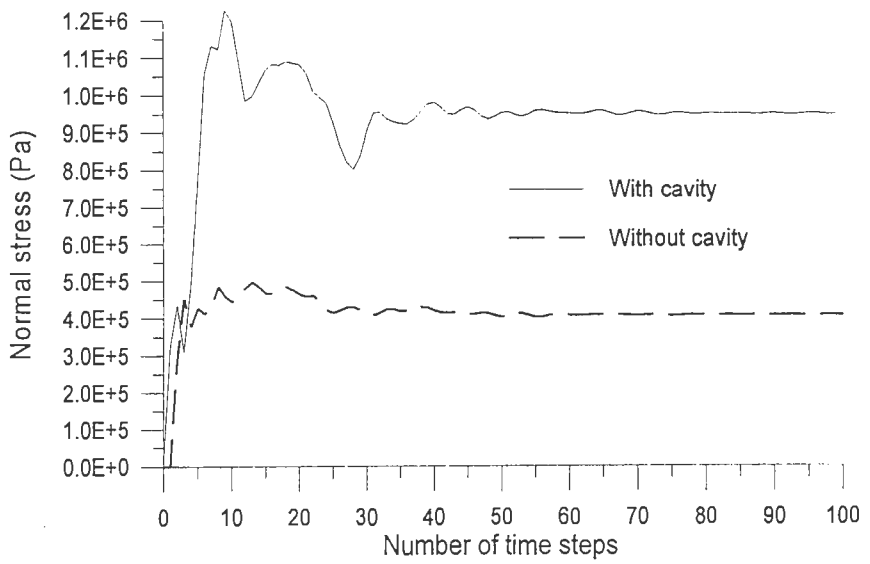

Figure 10a. Normal stress σ33 at point D.

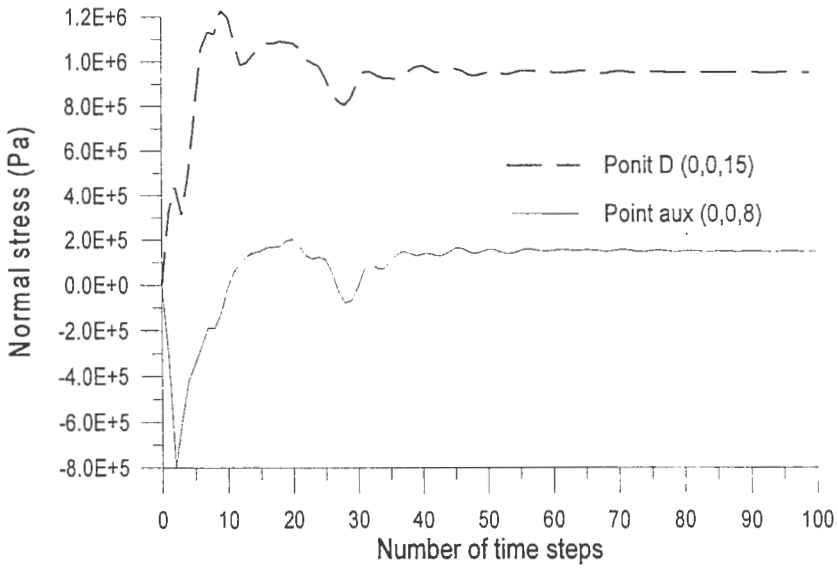

Figure 10b. Normal stress σ33 at points D and at an auxiliary point.

The sphere inclusion generates a small influence on the displacement analysis, as the load is extended to infinite, affecting mainly point D. Concerning the stress behavior, one can observe in figure 10a the stress concentration at point D. It occurs because point D is relatively near to the cavity bottom. In figure 10b it is possible to see that under the cavity there exist two situations. One can observe the "lens" effect at point D, which is placed at more than a diameter under the spherical cavity bottom. The spherical cavity presence amplifies the stress values. At the auxiliary point, placed near the bottom of the sphere, one can see the "shadow" effect; therefore the stress intensity is reduced.

Rigid Footing Subjected to Harmonic Loading

In this example the behavior of a rigid footing placed on a half space and subjected to a set of vertical harmonic loading is analyzed by the use of the time domain formulation. The footing is square with side length L=100cm. The half space is elastic and has the following properties: $E = 10^8 kg/m/s^2$, $\rho = 0.0016 kg/cm^3$ and $\nu = 0.25$. As, for this example the interest is only in surface values, the free surface is not discretized (see for instance Karabalis & Beskos(1984)). One bilinear boundary element was used to discretize the footing. Figures 11a, 11b and 11c show the time behaviour of the applied load and the vertical displacement of the footing for the frequencies 4000rad/s, 8000rad/s e 12000rad/s, respectively. The time step adopted is $\Delta t = 2{,}864 \times 10^{-5} s$.

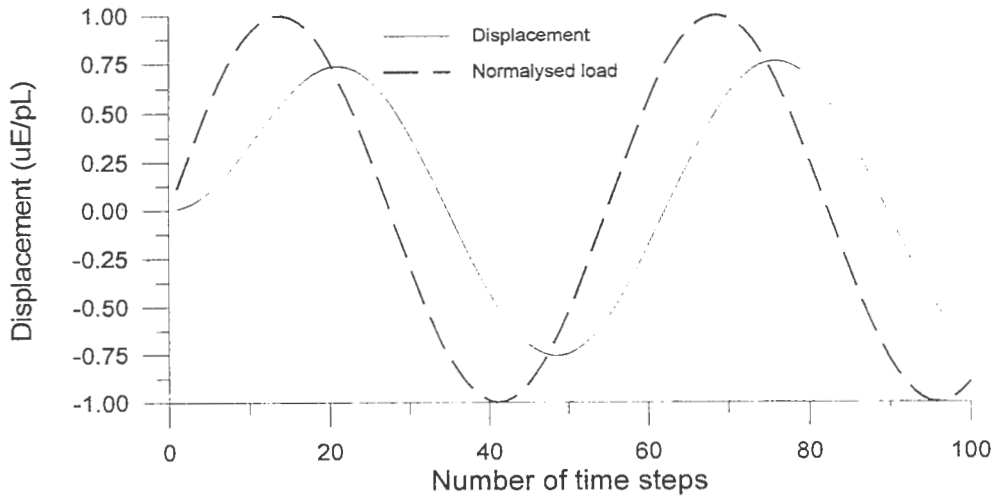

Figure 11a. Rigid footing vertical displacement for load frequency w = 4000 rad/s.

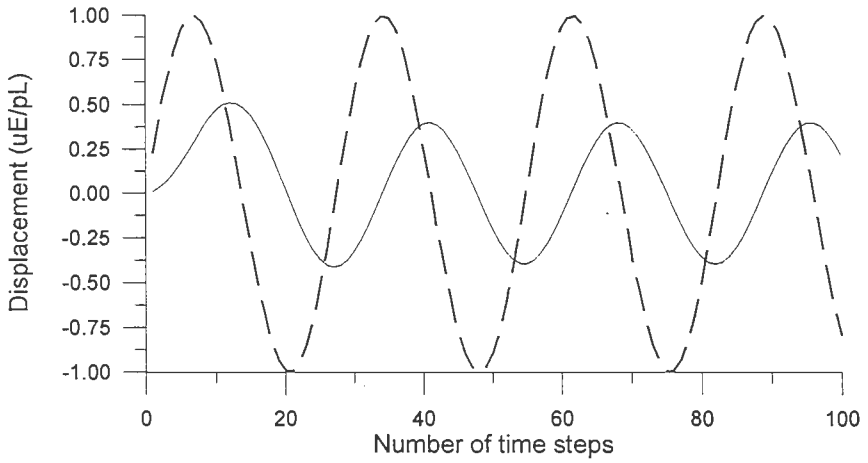

Figure 11b. Rigid footing vertical displacement for load frequency w = 8000 rad/s .

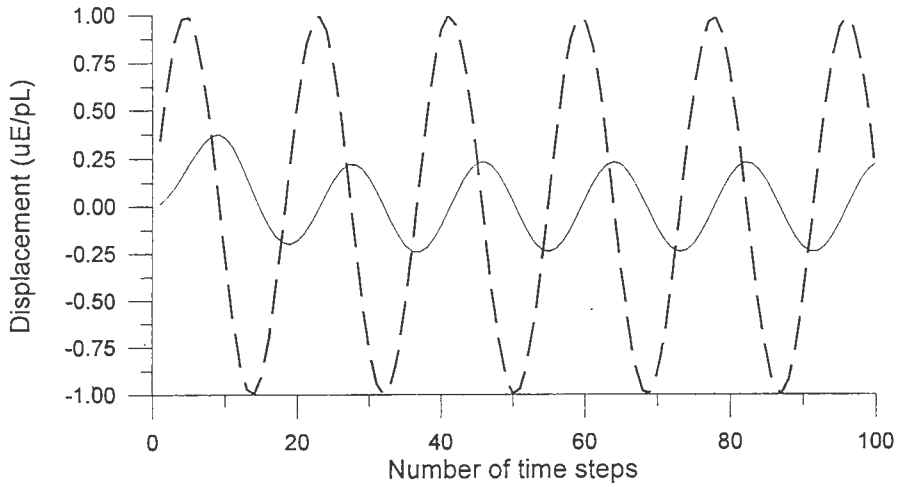

Figure 11c. Rigid footing vertical displacement for load frequency w = 12000rad/s.

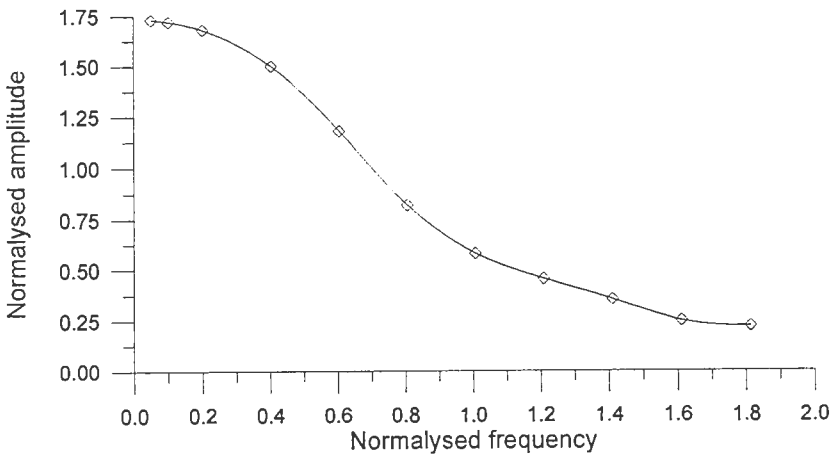

Figure 12. Amplitude for various load frequencies.

Figure 12 shows the vertical displacement amplitude versus load frequency values.

Displacement, amplitude and frequency normalization is carried out as $|u_z| = u_z E/(p L)$, $|a| = a E/(p L)$ and $|w| = w L/(2\pi C_2)$, respectively. It is worth observing the behavior of phase changes in the movement as frequency changes, figure 11. As a consequence of phase changes, the amplitude falls as the frequency increases. In order to obtain more results for larger frequency values it is necessary to improve the discretization.

Two Towers Connected to the Soil by Piles

Two towers placed near each other and connected to the soil by means of piles were analyzed when one of them is subjected to an external load, figure 13. For each tower five finite elements are adopted to model the buried part of the structure and ten to model the other part. A sudden horizontal load is applied and sustained for the rest of the analysis (Heaviside function), with $F_H = 4x10^6 kgdm/s^2$, see figure 13.

For this example a special fundamental solution is used. It is not as good as the complete Lamb's solution (Johnson (1974)) for the half space, but for this analysis it is sufficient. It consists of two Stokes' fields with one collocation point each. The first collocation point is placed at the real position, i.e., on the discretization nodal point, namely (x_1,x_2,x_3). The other collocation point is placed at the image of the real point related to the free surface, i.e., (x_1,x_2,x_3). The resulting field is achieved by subtracting the second value from the first one. Over the boundary and following Cauchy relation, the tangential surface forces are zero and the vertical one is non-zero. As the vertical one is less importante for the horizontal movement (analyzed one) this fundamental solution can be used in this analysis. The displacement fundamental values have no importance, as the real surface forces, for this example, are zero.

The adopted physical properties are:

Towers and piles:

$E = 2,1 X 10^9 kg/(dm.s^2)$, $\rho = 6 kg/dm^3$,

$A = 79\ dm^2$, $I = 491\ dm^4$.

Half space: $E = 2,6 X 10^7 kg/(dm.s^2)$, $\rho = 2 kg/dm^3$, $\upsilon = 0,33$

The displacement results are shown in figure 14 through 18.

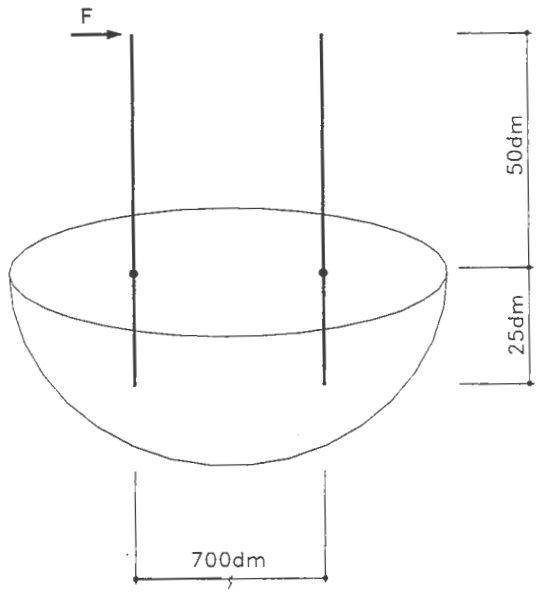

Figure 13. Towers connected to the soil.

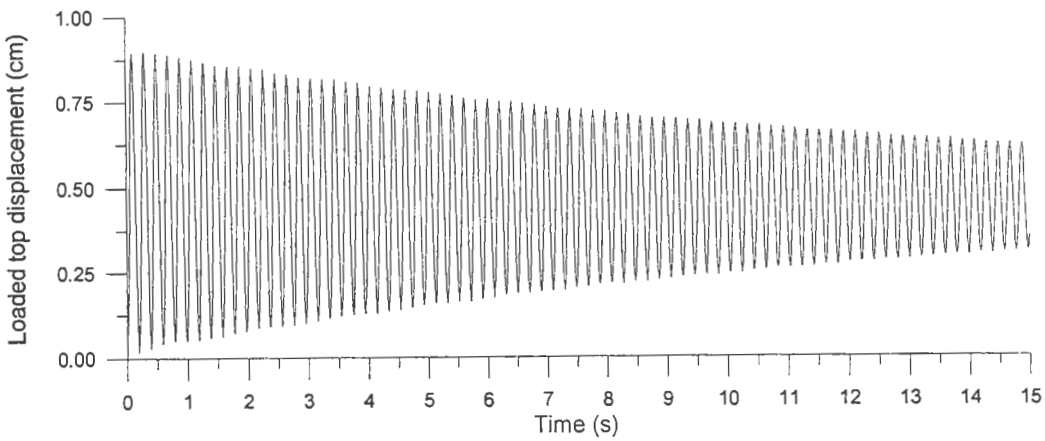

Figure 14. Loaded tower top displacement, long time analysis.

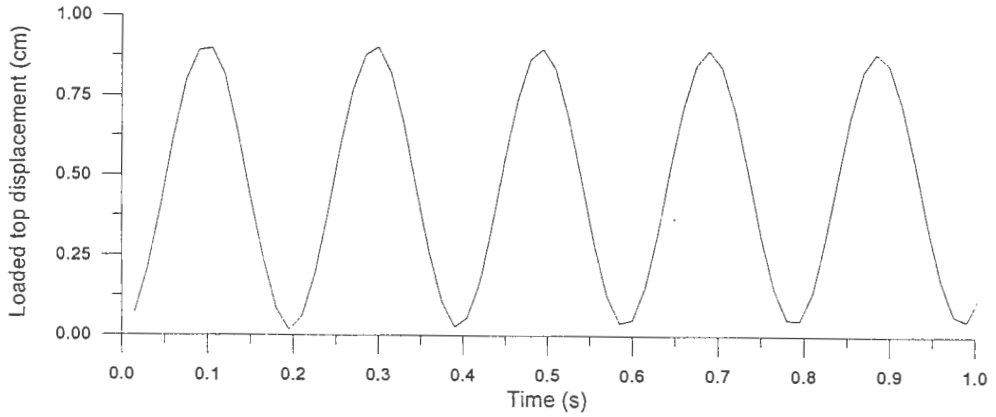

Figure 15. Loaded tower top displacement, short time analysis.

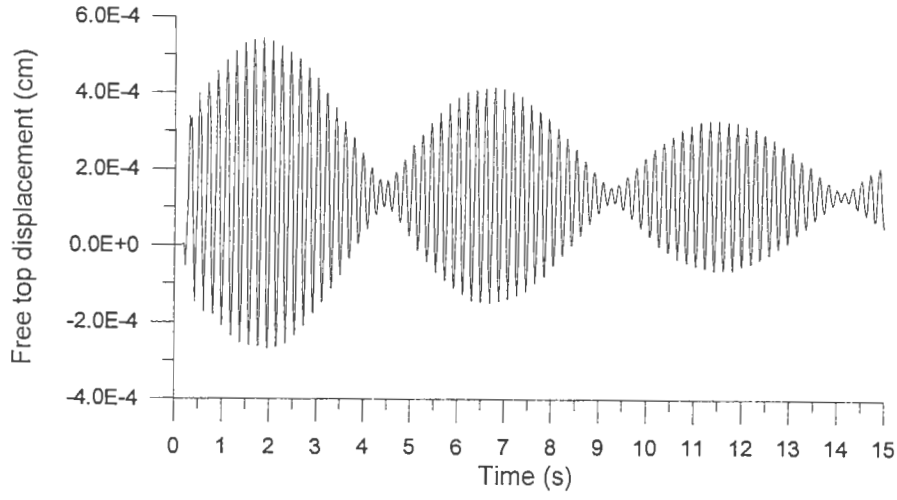

Figure 16. Free tower top displacement, long time analysis.

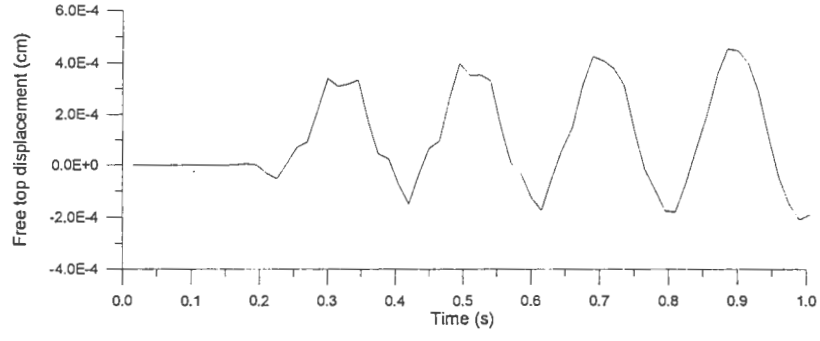

Figure 17. Free tower top displacement, short time analysis.

A very common phenomenon appears in this example, i.e., one can see in figure 16, that the movement amplitude of the free tower oscillates between a maximum and a zero value. This same behavior is verified for two concentrated masses connected by a spring. This movement leads to the conclusion that this formulation gives a complete solution. The time extension of the analysis shows that the process is quite stable even for long time analysis.

Conclusions

The Time Domain Boundary Element formulation has been presented in its most important aspects. A discussion about the integral kernels has brought suggestions to find the most appropriate approach to build stable and general formulations. A straightforward coupling formulation has been presented, as well as the correct form to adopt external collocation points, leading to the possibility of using non-singular TDBEM as an alternative approach. Three examples have demonstrated the good, general and stable behaviors of the formulation presented. Clues about the necessary care to use different schemes, namely CLI, LI and SLI have been given. These clues can help future researchers choose the most suitable technique for the application studied. Now it is possible to start other fields of studies such as viscoelasticity, anisotropy and crack growth in dynamics, using any desired fundamental solution and providing both accurate and stable results.

References

Antes, H. & Steinfeld, B.A., 1992, "Boundary Formulation Study Of Massive Structures Static And Dynamic Behaviour". In: BREBBIA, C.A. et alli eds., Boundary Elements XIV, Vol.2, 27-42, Comp. Mech. Pub. & Elsevier Sc. Pub.

Araujo, F.C. 1994, *Zeitberreichslösung linearer dreidimensionaler probleme der elastodynamik*

mit einer gekoppelten BE/FE - Methode. PhD Thesis, Technische Universität Brauschweig, Brauschweig, German.

Araujo FC, Mansur WJ, Nishikava LK (1999) "A linear theta time-marching algorithm in 3D BEM formulation for elastodynamics" Eng Anal Bound Elem 23: (10) 825-833 DEC 1999

Achenbach, J.D. (1973) *Wave propagation in elastic solids,* Amsterdan, North-Holand.

Bathe, K. J., 1982 *Finite element procedures in engineering analysis.* Englewood Cliffs, Prentice Hall.

Beer, G. & Watson, J. O., 1992 *Introduction to Finite and Boundary Element Methods for Engineers.* John Wiley & Sons, New York.

Beskos, D.E., 1987, Boundary element methods in dynamic analysis. *Appl. Mech. Rev.*, 40, 1-23.

Beskos, D.E, 1997, Boundary element methods in dynamic analysis: Part II (1986-1996). *App. Mech. Rev.*, 50, 149-197.

Carrer, J.A.M. & Mansur, W.J., 2001, "A time-domain boundary element formulation with fundamental solution generated by Heaviside function souce: Initial conditions contributions., in: *Advances in Boundary Element Techniques II,* Duda, M, Aliabadi, MH, Charafi, A. eds.

Carrer JAM, Mansur WJ, 1999 "Stress and velocity in 2D transient elastodynamic analysis by the boundary element method" Eng. Anal. Bound. Elem 23: (3) 233-245

Coda, H.B., 1993, "Three-dimensional transient analysis of structures by a BEM/FEM combination". Ph.D. Thesis, University of São Paulo (Br), (in Portuguese).

Coda. H.B. & Venturini, W.S., 1995a "Three dimensional transient BEM analysis". Computer & Structures, 56, 751-768.

Coda. H.B. & Venturini, W.S., 1995b, "Non-singular time-stepping BEM for transient elastodynamic analysis", Engineering Analysis with Boundary Elements, 15, 11-18.

Coda, H.B. & Venturini W.S., 1996a "A Smooth Fundamental Solution for 3D Time Domain BEM". In: BREBBIA C.A. et alli eds., Boundary Elements XVIII, Computational Mechanics Publications, 259-267.

Coda, H.B. & Venturini, W.S., 1996b, "Further improvements on three dimensional transient BEM elastodynamics analysis". Engineering Analysis with Boundary Elements, 17, 231-243.

Coda. H.B. & Venturini, W.S., 1996c, "A simple comparison between two 3D time domain elastodynamic boundary element formulations". Engineering Analysis with Boundary Elements, 17, 33-44.

Coda, H.B.; Venturini, W.S.; Aliabadi, M.H., 1999a, "A general 3D BEM/FEM coupling applied to elastodynamic continua/frame structures interaction analysis". International Journal for Numerical Methods in Engineering, v.46, n.5, p.695-712, Oct. 20.

Coda, H.B.; Venturini, W.S., 1999b, "On the coupling of 3D BEM and FEM frame model applied to elastodynamic analysis". International Journal of Solids and Structures, v.36, n.31-32, p.4789-4804, 1999.

Coda, H.B., 2000a "Contributions to the dynamic analysis of continuum by the boundary element method" Associate professor qualification text, EESC-USP, 2000 (in Portuguese)

Coda, H.B.2000b Discussions on the time domain integral representation for elastodynamic analysis [CD-ROM]. J.L. Tassoulas & D.R. Maniar edn. *Fourteen Engineering Mechanics Conference, American society of Civil Engineers (EM 2000)*, The University of Texas, Austin, May 21-24, 2000, -10p.

Domingues J., 1993 *Boundary Elements in Dynamics*, CM Pub., Southampton Elsevier Applied Science, London, U.K..

Johnson, L.R (1974)"Gren's function for Lamb's problem, *Geoph J. R. Astr. Soc., 37, 99-131.*

Eringen, A.C. & Suhubi, E.S., 1974, "Elastodynamics: linear theory". Academic Press, New York, London.

Karabalis, D.L. & Beskos, D.E., 1984, "Dynamic Response of 3-D Rigid Surface Foundations by Time Domain Boundary Element Method". Earth. Eng. Struct. Dyn., 12, 73-93.

Kobayashi, S. 1987, "Elastodynamics". In: BESKOS, D.E., ed., Boundary element methods in mechanics. North Holland, Amsterdam, 191-255.

Love AEH, 1944, A treatise on the mathematicl theory of elasticity, a ed, New Your Dover.

Manolis, G.D. et alli., 1986, "Boundary element method implementation form three - dimensional transient elastodynamics". in: Banerjee, P.K. and WATSON, J.O. eds., Developments in boundary element methods - 4. London, Elsevier, 29-65, 1986.

Mansur W.J. & Brebbia C.A. 1985, "Transient Elastodynamics", In: Brebbia C.A. Eds, Topics in Boundary Element Research, V2.

Mansur, W.J., 1988, "Boundary element method applications in two-dimensional transient elastodynamics". In: BREBBIA, C.A., ed., Boundary elements X. Southampton, Springer-Verlag, Berlin, Vol.4, 387-399.

Mansur, WJ, Yu GY, Carrer, JAM, 2000, "The θ scheme for time-domain BEM/FEM coupling applied to the 2-D scalar wave equation. *Commun. Numer. Meth. En.* 16, (6), 439-448.

Risos D.C. & Karabalis D.L., 1997, "A time domain BEM for 3-D Elastodynamic Analysis Using B-Spline Fundamental Solutions", IABEM97, Spain.

Siebrits, E. & Peirce, A.P., 1997, "Implementation and application of elastodynamic boundary element discretizations with improved stability properties", Engineering Computations, 14, 669-691.

Sladek, V. & Sladek, J., 1992, "Time marching analysis of boundary integral equations in two-dimensional elastodynamics". Engineering Analysis with Boundary Elements, 9, 21-29.

Stokes, G. G., 1849 "On the dynamical theory of diffraction." Transactions of the Cambridge Philosophical Society, v.9, p.1.

Wheeler L.T. & Sternberg E., 1968, "Some theorems in classical elastodynamics". Archive for Rational Mechanics and Analysis, 31, 87-90.

Yu G, Mansur WJ, Carrer JAM , 1999 "The linear theta method for 2-D elastodynamic BE analysis" *Comput. Mech,* 24: (2) 82-89 .

